RESEARCH LETTER – Environmental Microbiology

Microbial activity during a coastal phytoplankton bloom on the Western Antarctic Peninsula in late summer

María E. Alcamán-Arias[1,2,3], Laura Farías[1,3], Josefa Verdugo[4], Tomás Alarcón-Schumacher[2] and Beatriz Díez[2,3,*]

[1]Department of Oceanography, Universidad de Concepción, 4070386 Concepción, Chile, [2]Department of Molecular Genetics and Microbiology, Pontificia Universidad Católica de Chile, 6513677 Santiago, Chile, [3]Center for Climate and Resilience Research (CR)[2], Universidad de Chile, 8370448 Santiago, Chile and [4]Alfred-Wegener-Institute Helmholtz-Centre for Polar and Marine Research, 27570 Bremerhaven, Germany

*Corresponding author: Department of Molecular Genetics and Microbiology, Faculty of Biological Sciences, Pontificia Universidad Catolica de Chile, Libertador Bernardo O´Higgins 340, Casilla 144-D, C.P. 6513677 Santiago, Chile. Tel: +5623542661; E-mail: bdiez@bio.puc.cl

One sentence summary: Microbial activities in the marine Antarctic C and N cycles.

Editor: Jean-Claude Piffaretti

ABSTRACT

Phytoplankton biomass during the austral summer is influenced by freezing and melting cycles as well as oceanographic processes that enable nutrient redistribution in the West Antarctic Peninsula (WAP). Microbial functional capabilities, metagenomic and metatranscriptomic activities as well as inorganic ^{13}C- and ^{15}N-assimilation rates were studied in the surface waters of Chile Bay during two contrasting summer periods in 2014. Concentrations of Chlorophyll *a* (Chl*a*) varied from 0.3 mg m^{-3} in February to a maximum of 2.5 mg m^{-3} in March, together with a decrease in nutrients; however, nutrients were never depleted. The microbial community composition remained similar throughout both sampling periods; however, microbial abundance and activity changed with Chl*a* levels. An increased biomass of Bacillariophyta, Haptophyceae and Cryptophyceae was observed along with night-grazing activity of Dinophyceae and ciliates (Alveolates). During high Chl*a* conditions, HCO_3^- uptake rates during daytime incubations increased 5-fold (>2516 nmol C L^{-1} d^{-1}), and increased photosynthetic transcript numbers that were mainly associated with cryptophytes; meanwhile night time NO_3^- (>706 nmol N L^{-1} d^{-1}) and NH_4^+ (41.7 nmol N L^{-1} d^{-1}) uptake rates were 2- and 3-fold higher, respectively, due to activity from Alpha-/Gammaproteobacteria and Bacteroidetes (Flavobacteriia). Due to a projected acceleration in climate change in the WAP, this information is valuable for predicting the composition and functional changes in Antarctic microbial communities.

Keywords: Antarctic microbial communities; phytoplankton bloom; bacterioplankton; C and N assimilation pathways; metatranscriptomics

INTRODUCTION

The Southern Ocean (SO) plays a substantial role in regulating the global climate, as it sequesters ∼40% of global CO_2 (Sabine *et al.* 2004; Takahashi *et al.* 2009; Frölicher et al. 2016), principally through phototrophic activity (Metzl, Tilbrook and Poisson 1999; Takahashi *et al.* 2009; Deppeler and Davidson 2017). Therefore, changes or disturbances in the SO may produce an unquantified effect on the carbon (C) cycle. The Western Antarctic Peninsula (WAP) is known to be the region with the most extreme changes in the Southern Hemisphere, and has undergone substantial warming over the last 50 years. Although the rate of atmospheric temperature increase in the WAP has recently been shown not to increase further (Turner *et al.* 2016), since 1951 it has already risen by nearly 3°C (Meredith and King 2005; Steig *et al.* 2009; Ducklow *et al.* 2012).

Thus, marine ecosystems in the SO are driven to biologically adapt due to permanent disturbances as a result of climate change (Montes-Hugo *et al.* 2009). For example, sea ice cap retreat increases light penetration and the release of metals and some other nutrients (Statham, Skidmore and Tranter 2008; Hawkings et al. 2014; Wang *et al.* 2014), enhancing bioavailability and increasing stratification in the water column due to surface water freshening (Ducklow *et al.* 2013). These conditions could favour the development of large algal blooms (Vernet *et al.* 2008; Borges-Mendes, Silva de Souza and Tavano Garcia 2012; Giovannoni and Vergin 2012; Rozema *et al.* 2017b), resulting in high carbon uptake within coastal waters (Cavicchioli 2015; Bunse and Pinhassi 2017). On the contrary, reduced sea ice cover may provoke a deepening of the mixed layer caused by wind action, promoting a reduction in phytoplankton biomass (Montes-Hugo *et al.* 2008) and productivity, shifting the composition from mainly diatoms to cryptophytes and other small flagellates (Walsh, Dieterle and Lenes 2001; Moline *et al.* 2004; Ducklow *et al.* 2007; Borges-Mendes *et al.* 2013; Kavanaugh *et al.* 2015; Schofield *et al.* 2017). Considering the ubiquity and important contribution of diatoms to global primary carbon fixation (up to 25%) (Field *et al.* 1998), fluctuations in their global production, influenced by climate change, may affect carbon transport to deeper layers (Korb *et al.* 2010).

Furthermore, climate-induced modifications to the structure and/or function of phytoplankton communities may alter the efficiency of the biological pump, affecting feedback mechanisms related to climate change (Le Quéré *et al.* 2007). Since phytoplankton blooms are dependent on the WAP's physicochemical and climatic factors, global warming is predicted to trigger substantial modifications to bloom structure and distribution. In addition, this will influence bacterioplankton dynamics (Rozema *et al.* 2017b), as well as primary productivity and other processes involved in the biogeochemical cycle (Ducklow *et al.* 2007, Deppeler and Davidson 2017, Schofield *et al.* 2017).

In summer, Antarctic waters are dominated by the following: eukaryotic oxygenic photoautotrophs, including large (>20 μm) and small (<20 μm) diatoms and small flagellates (pico- and nanoplankton, <20 μm), such as prasinophytes, haptophytes, cryptophytes (Prézelin *et al.* 2000; Varela *et al.* 2002; Garibotti, Vernet and Ferrario 2005; Ducklow *et al.* 2012; Schofield *et al.* 2017); mixotrophic eukaryotes (Kopczyńska, Fiala and Jeandel 1998; Moorthi *et al.* 2009; McKie-Krisberg, Gast and Sanders 2015); and prokaryotic chemoheterotrophs and photoheterotrophs, including aerobic anoxygenic phototrophs (Grzymski *et al.* 2012; Kirchman *et al.* 2014; Gonçalves-Araujo *et al.* 2015; Egas *et al.* 2017). The combined activities of these microorganisms guarantee active carbon (C) and nitrogen (N) recycling within the trophogenic zone, as well as support food webs (Piquet *et al.* 2011, Schofield *et al.* 2017), influence air-sea gas exchange, and play a major role in atmospheric chemistry and climate (Hallegraeff 2010; Schmale et al. 2013).

In previous decades, the loss of the ice shelf of coastal glaciers around the Antarctic Peninsula has left exposed an area of open water that exceeds 2.4 × 10^4 km^2. This in turn enables new phytoplankton blooms, which act as carbon sink and lead to a negative feedback to the climate (Peck *et al.* 2010). Moreover, the increase in photosynthetic biomass stimulates microbial community activity (Ducklow *et al.* 2012), including eukaryotic grazers and mixo- and hetero-trophic bacteria (Wilkins *et al.* 2013; Buchan *et al.* 2014; Delmont *et al.* 2014). Thus, bacterioplankton abundance and composition are influenced by changes in the abundance and composition of phytoplankton blooms (Williams *et al.* 2013; Luria *et al.* 2016; Evans *et al.* 2017).

Changes in microbial cell size, abundance, composition and activity might also affect the assimilation and recycling rates for N and other bioelements (Finkel *et al.* 2010). High NO_3^- (>10 mmol N m^{-3}) and low NH_4^+ (i.e. generally 0.1 mmol N m^{-3}) concentrations have been reported throughout the WAP, for example in the Bransfield Sea (Bode *et al.* 2002); however, high NO_3^- assimilation rates are not maintained consistently high; meanwhile, NH_4^+ is used as a nitrogen source (Olson 1980; Koike, Holm-Hansen and Biggs 1986; Waldron *et al.* 1995, Joubert *et al.* 2011; Bode *et al.* 2002). Recently, Pearson *et al.* (2015) used metatranscriptomics on diatom-rich communities in contrasting coastal habitats of the WAP, and revealed a functional differentiation in nutrient acquisition; specifically, that NH_4^+ and urea were the most important forms of reduced N, despite the apparent abundance of NO_3^- in the water column. However, during productive periods, such as a bloom event, N assimilation activities, such as NO_3^- and a NH_4^+ uptake, are poorly understood.

Metagenomics, metatranscriptomics and *in situ* experiments using stable isotopes ^{13}C and ^{15}N were carried out in the coastal waters of Chile Bay in the WAP. This study improves knowledge on the major C and N assimilation processes driven by active microbial communities, over distinct periods during the austral summer with varied environmental conditions and Chl*a* concentrations. Also, the location is directly affected by freshwater and particle (e.g. trace metals) input into the marine system due to the deglaciation of surrounding glaciers. This study area represents a typical glacial retreat scenario for a bay within Greenwich Island (Santana and Dumont 2002; Petlicki and Kinnard 2016). The reported trend corresponds to future climate scenarios, including significant sea ice reduction (Arblaster, Meehl and Karoly 2011; Fan, Deser and Schneider 2014). This study provides valuable information on energy flow predictive models in changing systems, such as the regions that are threatened by accelerated climate change.

MATERIAL AND METHODS

Sample site and collection

Surface (2 m) seawater samples were collected from Chile Bay (62°27'6' S; 59°40'6" W), Greenwich Island, South Shetland Island, Antarctica (Fig. 1). Samples were taken during the following dates and times of day; nocturnal on 11 February and 4 March; diurnal on 14 February and 3 March 2014. The aim was to investigate and compare the microbial communities present during two contrasting summer periods, with different environmental conditions and Chl*a* levels. Near-surface water was pumped using a hand-operated membrane pump aboard the
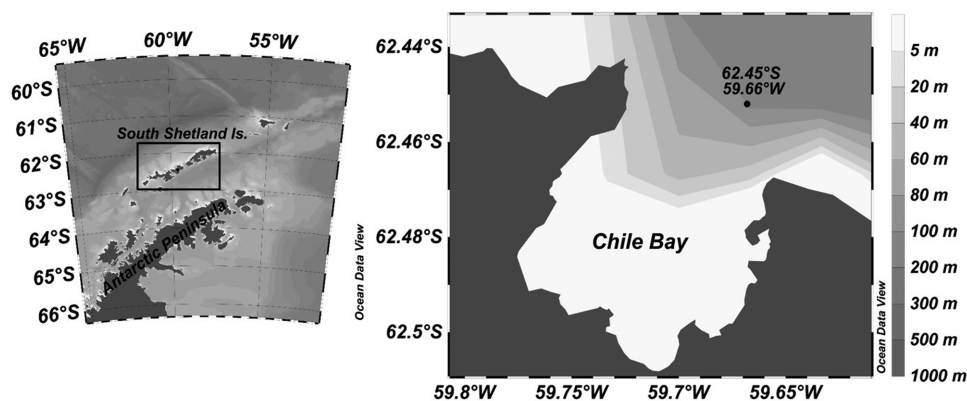
Figure 1. Map of Chile Bay, Greenwich Island, South Shetland Island, Antarctica. The dot indicates the near surface seawater sample point, sampled during February and March 2014.

small inflatable boat; samples were deposited into 20-L clear bottles that had been cleaned with HCl 10%; samples were then transported to the INACH (INstituto Antártico CHileno) laboratory at Chile Bay for sample processing and assays.

Environmental variables

During the sampling period, variables such as temperature, salinity and oxygen were measured using a multiparameter sensor (OAKTON PCD650). To determine NO_2^-, NO_3^-, PO_4^{3-} and $Si(OH)_4$ nutrients, seawater samples were collected in 15-ml polyethylene flasks, and stored at –20°C until further analysis. The WOCE protocol was followed (https://www.nodc.noaa.gov/woce/woce_v3/wocedata_1/whp/manuals/pdf/91_1/gordnut.pdf). The analysis was conducted using standard colorimetric techniques in a segmented flow Seal AutoAnalyser (Seal Analytical AA3). The $NO_3^- + NO_2^-$ (detection limit 0.05 μM) and PO_4^{3-} (detection limit 0.02 μM) were measured at submicromolar levels according to v (1967), whereas $Si(OH)_4$ (detection limit 0.65 μM) was measured according to Thomsen, Johnson and Petty (1983). For Chl*a* determination, 1 L of seawater was filtered through a 0.7-μm GF/F glass fibre filter, and samples were frozen until acetone extraction and fluorometric determinations were conducted following Strickland and Parsons (1972). For NH_4^+ determination, samples were collected in glass flasks and analysed as described by Solorzano (1969) with a detection limit of 0.05 μM.

0.1 and ^{15}N assimilation assays and rate determinations

To determine the isotopically-labelled assimilation of carbon and nitrogen, dual injections of ^{13}C and ^{15}N tracers were carried out in duplicate in polycarbonate bottles (0.58 L), during both sampling periods and under light and dark incubation conditions. For C uptake, 0.5 ml of $H^{13}CO_3$ was added (3.645 mg ^{13}C ml^{-1}, equivalent to 0.5 μmoles ml^{-1}), corresponding to ~10% enrichment according to natural DIC concentrations reported for the coastal WAP (Hauri *et al.* 2015). For N uptake, $^{15}NH_4Cl$ (99% at 0.5 μmol ml^{-1}) and $K^{15}NO_3^-$ (99% at 0.5 μmol ml^{-1}) were added in doses that ensured <10% enrichment considering natural concentrations, following data in Slawyk and Raimbault (1995). Independent of sampling time (i.e. February or March), light (uncovered bottles) and dark (covered bottles) incubations were performed. All bottles were incubated at Chile Bay pier for 24 h, at 1 m depth under *in situ* conditions. Subsequently, samples

were filtered through gentle vacuum filtration (<100 mm Hg) through pre-combusted GF/F glass fibre filters. Filters were dried at 60°C and stored until analysis by continuous-flow isotopic ratio mass spectrometry (Finnigan Delta Plus IRMS, Universidad de Concepción) (Fernandez, Farías and Alcamán 2009).

Daily rates of autotrophy were expressed as mg L^{-1} d^{-1} according to Raimbault *et al.* (1999):

$$\rho DI\,^{13}C = \left[\frac{(\%R_{POC} - R_n)* \left(\frac{POC}{12*V_f} \right)}{\%R_{DIC}} \right]^* 12 \quad (1)$$

$$\%R_{DIC} = \left[\frac{\left(\frac{V^{13}C*^{13}DIC}{V_b} \right) + DIC_i^{*0.01112}}{DIC_i - \frac{V^{13}C*^{13}DiC}{V_b}} \right]^* 100 \quad (2)$$

where V_f represents the filtered volume and POC (in μg) is the amount of particulate organic carbon recovered from the filter after incubation, and measured by mass spectrometry. $\%R_{DIC}$ indicates excess tracer enrichment following inoculation (To), calculated using Equation (2). $\%R_{POC}$ is the ^{13}C enrichment in the filter after incubation, as measured by the tracer mass. In Equation (2), $V^{13}C$ is the volume of ^{13}C added to the sample during inoculation, while ^{13}DIC accounts for the tracer concentration added to the sample (3.6456 mg ^{13}C ml^{-1}). DIC_i represents the initial amount of DIC in the sample. V_b is the volume in the incubation bottle (0.58 L).

Rates of NH_4^+ (ρNH_4^+) and NO_3^- (ρNO_3^-) assimilation were determined by estimating the transport rate of ^{15}N-labelled DIN from the DIN pool to the PON pool, and the net DIN uptake (ρDIN, nmole L^{-1} d^{-1}) was calculated according to the following equation (Dugdale and Wilkerson 1986):

$$\rho DIN = \frac{R_{PON}}{R_{DIN} \times t} \times [PON] \quad (3)$$

where R_{PON} and R_{DIN} represent percentage of excess enrichment of ^{15}N in the PON and DIN pools, respectively, [PON] represents the final PON concentration, and t represents the duration (h) of incubation.

DNA and cDNA extractions

Microbial biomass for DNA and cDNA analysis, from diurnal and nocturnal samples collected over the two periods (with different Chl*a* levels), were concentrated onto 0.22-μm pore size Sterivex

units (Durapore; Millipore), achieved by prefiltering 3–4 L of near surface seawater (2 m depth) through a 200-μm nylon mesh followed by a 20-μm polycarbonate filter using a Cole Palmer System peristaltic pump Model no. 7553–70 (6–600 rpm), at 50–100 ml min^{-1}. The RNA filters were preserved in RNAlater and maintained at –80°C with the DNA filters (one day and one night per sampling period) until later analysis in the laboratory (at Pontifical Catholic University of Chile).

DNA was extracted according to a modified protocol described in Díez, Pedrós-Alió and Massana (2001). Briefly, filters were resuspended in lysis buffer (10 mM Tris-HCl pH = 8.0, 1 mM EDTA, 0.15 M NaCl, 1% sodium dodecyl sulphate, 0.1 mg ml^{-1} Proteinase K) and sterile glass beads. The mix was incubated at 37°C for 1 h with vortex mixing every 15 min. NaCl and cetrimonium bromide were added to reach a final concentration of 0.6 M and 1%, respectively, and the mix was incubated at 65°C for 10 min. DNA was extracted with phenol-chloroform-isoamyl alcohol (25:24:1), and the residual phenol was eliminated with chloroform-isoamyl alcohol (24:1). The extract was cleaned up by two successive precipitations with cold isopropanol and 70% ethanol. Nucleic acids were quantified using the Qubit® 2.0 Fluorometer (Thermo Fisher Scientific, Inc.), quality was assessed by spectrophotometry (A260/A280 ratio) and integrity by standard agarose gel electrophoresis. A set of 2 RNA samples (from 14 February and 4 March) were extracted using the Qiagen Kit, according to the manufacturer's specifications, and two additional RNA samples (from 11 February and 3 March) were extracted using TRIzol® (Invitrogen) and the RNA Clean & Concentrator kit (Zymo Research, USA). The quality and quantity of the total extracted RNA was determined using a Qubit® 2.0 Fluorometer (ThermoFisher Scientific, Inc.), and the integrity was checked by electrophoresis in an RNase-free 1% agarose gel. DNase treatment (TURBO, Applied Biosystems, USA) was performed on 1 μg of RNA from all samples to eliminate any remaining DNA.

Total DNA (20 ng ml^{-1}) and RNA (1 μg) from February 14 (day) and March 4 (night) were sequenced by Illumina Hi-Seq technology (DNA Sequencing & Genotyping Center, Delaware, USA). Briefly, DNA libraries were prepared using a NEXTflex Rapid DNA-Seq kit from Bio Scientific, while total RNA was first depleted of ribosomal RNA using RiboZero and RNAseq libraries; then samples were prepared using a NEXTflex Rapid Directional RNA-Seq kit from Bio Scientific. Additionally, RNA from 11 February (night) and 3 March (day) were sequenced by Illumina Hi-Seq technology (Roy J. Carver Biotechnology Center, Illinois), and rRNA was removed using a Ribozero kit (Illumina). The RNAseq libraries were prepared with Illumina's 'TruSeq Stranded mRNAseq Sample Prep kit' (Illumina). The libraries were quantitated by qPCR and sequenced on one lane for 151 cycles from one end of the fragments on a Hi-Seq 4000 using a Hi-Seq 4000 sequencing kit version 1. FastQ files were generated and demultiplexed with the bcl2fastq v2.17.1.14 conversion software (Illumina). Reads of 150 nt in length were obtained.

High-throughput sequencing analysis

Quality assessment and trimming
Briefly, a quality assessment of metagenomic and metatranscriptomic data was performed with the software FastQC (Andrews 2010). Quality trimming of sequences was performed with Cutadapt software (Martin 2011), with a hard clip of the first five and nine bases of 5′ for metagenomic and metatranscriptomic samples, respectively, and quality trimming of the 3′ with a minimum quality of 30. Additionally, sequences with N were discarded to avoid ambiguity in assignation. To retrieve reliable protein information, a minimum cut-off length of 30 bp was established.

For the metatranscriptomic data, the remaining rRNA sequences were removed using SortMeRNA (Kopylova, Noé and Touzet 2012). Primarily, the Silva database version 128 SSU and LSU (Quast *et al.* 2013), and the Rfam 5 s and 5.8 s databases were indexed to remove the maximum rRNA sequences, then, each sample was filtered with all indices and other parameters. Only non-aligning reads were considered for further analyses.

Taxonomic and functional profiles
To generate the taxonomical and functional profiles of each sample, alignment with Diamond v8.1 (Buchfink, Xie and Huson 2015) against the NCBI non-redundant protein database was carried out, with a maximum e-value of 1e-10 and a minimum score of 50. Then, the resulting alignment was presented using the lowest common ancestor algorithm implemented in MEGAN 6 (Huson *et al.* 2007), with a minimum score of 50 and default parameters. Functional assignation was carried out using the NCBI-taxonomic mapping file and the SEED, eggNOG and Interpro functional databases. All files from metagenomes and metatranscriptomes are deposited in NCBI as BioProject SUB3293570.

Statistical analysis

Between sampling periods, differences in biomass (measured as Chl*a*), uptake rates and differential expression of normalised counts of metatranscriptomic assigned reads (retrieved from Megan) were calculated using R (R Core Team) package DESeq (Anders and Huber 2010), following the established procedures. The threshold value for statistical difference was set as $P < 0.05$. To uptake experiments, an ANOVA one-way test was carried out to determine statistical difference between samples.

RESULTS

Environmental parameters

Table 1 presents the environmental variables obtained from a fixed location in Chile Bay (Fig. 1) during February and March of 2014. From February to March, seawater temperature increased from –0.1°C to 0.3°C, and salinity from 33.1 to 33.9, respectively. Additionally, air temperature increased during the sampling period from –2 to 2 °C, as well as wind speed and gusts (mainly N-NE: 58%) (Fuentes *et al.* submitted). Chl*a* concentrations increased significantly ($P < 0.009$) from relatively low values (0.31 mg m^{-3}) in February to a 7-fold increase (2.53 mg m^{-3}) in March. This rise in biomass coincides with an increase in oxygen saturation (i.e. from 151% in February to 190% in March), probably associated with photosynthetic activities. In general, nutrient concentrations (mainly NO$_3^-$ and HPO$_4^{2-}$) decreased slightly at the end of the sampling period, when the Chl*a* concentration reached its maximum. Concentrations of nutrients in February and March also decreased from 22.4 to 17.7 μM for NO$_3^-$, from 1.86 to 1.28 μM for HPO$_4^{2-}$ and from 46.8 to 37.9 μM for Si(OH)$_4$; however, NH$_4^+$ maintained submicromolar concentrations. N:P ratio values (between 12.1 and 13.9) were slightly lower than the expected Redfield ratio (16:1) (Redfield 1958), demonstrating that the system is not N limited (Table 1). The low N:Si ratio (0.451:0.482) denoted the high availability of Si(OH)$_4$.

Table 1. Environmental variables obtained from a predetermined location in Chile Bay during February and March 2014.

Date	Time	Depth (m)	Temperature (°C)	Salinity	O2 (%)	Chla (mg m-3)	NO2- (μM)	NO3- (μM)	PO4- (μM)	Si(OH)4 (μM)	N:P	N:Si
11.02.14	Night	3	−0.1	33.1	151	0.31	0.166	22.4	1.86	46.8	12.1	0.482
14.02.14	Day	3	−0.1	33.2	149	0.36	0.155	19.5	1.61	43.6	12.2	0.451
03.03.14	Day	3	0.3	33.5	168	2.38	0.160	20.2	1.59	44.1	12.8	0.462
04.03.14	Night	3	0.3	33.9	190	2.53	0.098	17.7	1.28	37.9	13.9	0.469
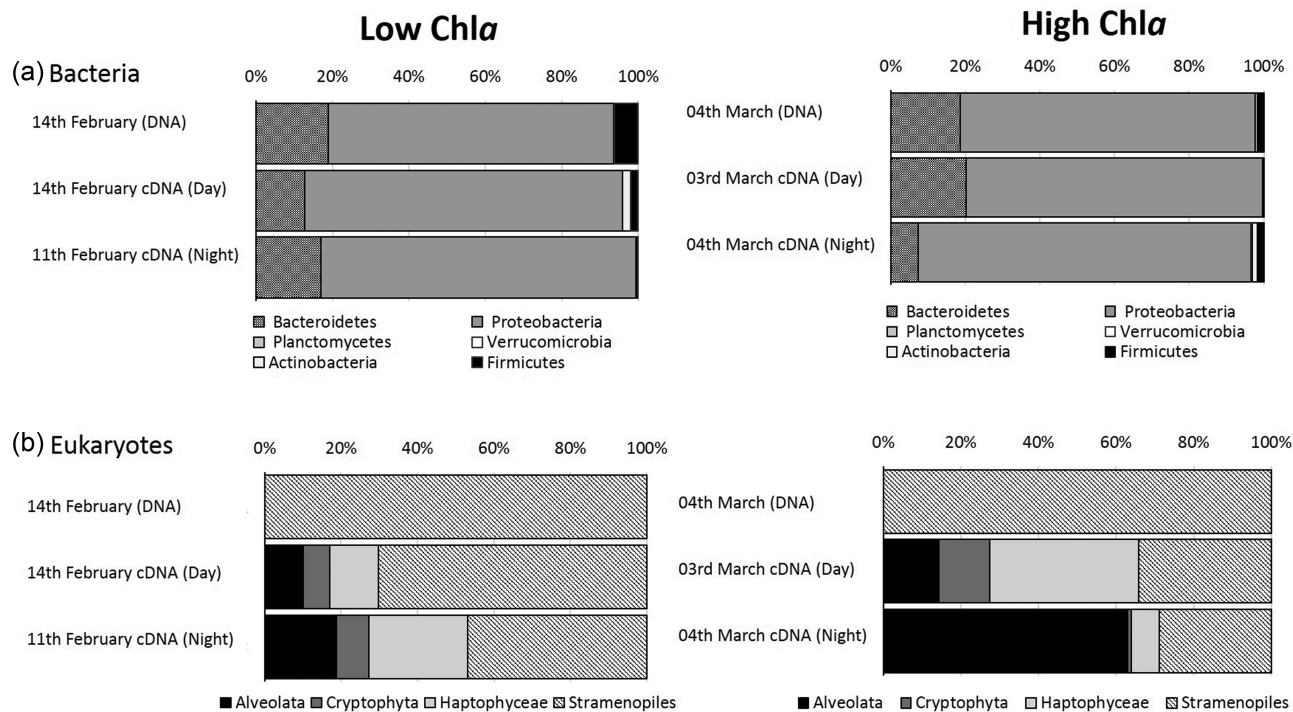
Figure 2. (a) Bacteria and (b) Eukaryotic abundance and transcript numbers during both sampling periods, in Chile Bay. Bacteria were predominantly represented by Proteobacteria and Bacteroidetes; meanwhile Eukaryotes were represented by Stramenopiles, Haptophytes, Cryptophyta and Alveolates.

Microbial community structure, composition and transcriptional expression

Metagenomic analyses showed that Bacteria were consistently more abundant than eukaryotes over both sampling periods with different Chl*a* levels (Supplementary Data, Fig. S1a); however, metatranscriptomics showed that eukaryotes were the most active microorganisms, attaining up to 35% and 70% of the total transcript numbers obtained over the two contrasting periods (Supplementary Data, Fig. S1b). Conversely, Archaea, represented mostly by Thaumarchaeota, attained ≤0.2% of the total relative abundance (including Bacteria, Archaea and Eukaryots) from metatranscriptomic transcript reads, indicating no difference between the two periods.

For Bacteria, Proteobacteria and Bacteroidetes phyla presented a greater relative abundance and activity during summer, with no daily variation in composition, and a slight increase (P < 1) in the total transcript numbers obtained during period of increased Chl*a* or bloom event (Supplementary data, Fig. S2a). During the increased Chl*a* period, Alphaproteobacteria, such as *Roseobacter*, Candidatus *Pelagibacter* and *Planktomarina*, and Gammaproteobacteria, such as *Alteromonas*, *Marinobacterium*, *Pseudoalteromonas* and Oceanospirillales, were observed more frequently (Supplementary Data, Fig. S2a). Dur-

ing the period of lower Chl*a*, changes in diurnal and nocturnal transcript abundance were observed for Alphaproteobacteria and Gammaproteobacteria. During the period with higher Chl*a*, similar diurnal patterns were observed (Supplementary Data, Fig. S2a). Furthermore, Bacteroidetes, specifically dominated by Flavobacteriia and *Polaribacter*, were always dominant and active at daytime throughout both sample periods (Supplementary Data, Fig. S2b).

Haptophytes (Isochrysidales, Phaeocystales and Prymnesiales) were quite active eukaryotes during both periods, with an average of 19.3% and 22.8% of the total abundance of transcriptomic reads, respectively (Fig. 2b; Supplementary Data, Fig. S3b). Stramenopiles mainly represented by Bacillariophyta accounted for 58.6% and 31.5% of the total abundance of transcriptomic reads, respectively (Fig. 2b; Supplementary Data, Fig. S3a). Specifically, Bacillariophyta were represented by small diatoms, such as *Fragilariopsis* and *Thalassiosira*, demonstrating similar activities throughout different productive periods (Supplementary Data, Fig. S3a). During the period of lower Chl*a*, diatoms reached 70.2% of the total eukaryotic transcripts in diurnal sampling, accompanied by minority groups, such as cryptophytes (*Teleaulax/Guillardia*: 6.8%), alveolates (*Stichotrichia*: 10.1%) and haptophytes (12.8%) (Fig. 2b). During this period, haptophytes were

Low Chl*a*

High Chl*a*
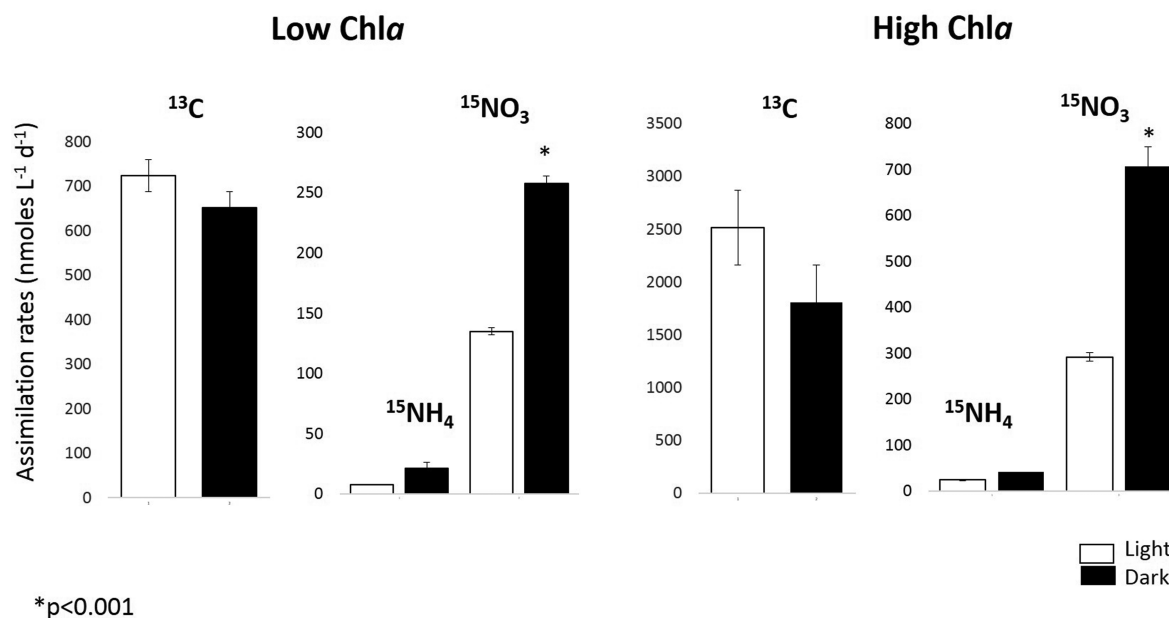
Figure 3. Recorded daily uptake rate of carbon (H^{13}CO$_3$), ammonium (^{15}NH$_4$Cl) and nitrate (K^{15}NO$_3$) under *in situ* conditions throughout the 2014 summer sampling period, in Chile Bay, considering high and low Chl*a* events. The white bars represent incubations exposed to light, and black bars the incubations maintained in darkness. Error bars represent duplicate replicates.

mainly represented by Phaeocystales (84.6%) and primarily dominated by the genus *Phaeocystis* (Supplementary Data, Fig. S3b). In contrast, the number of diatom-related transcripts in nocturnal samples was reduced to 46.9%, while haptophytes transcript numbers increased to 25.8% (Fig. 2b; Supplementary Data, Fig. S3), with shared activity by Isochrysidales (31.8%) (e.g. *Emiliania*), Phaeocystales (38.0%) (e.g. *Phaeocystis*) and Prymnesiales (30.2%) (e.g. *Chrysochromulina*). Another highly active nocturnal group was the alveolates (Ciliophora and Dinophyceae), which almost doubled (18.8%) their transcript abundance numbers compared to daytime (Fig. 2b).

Throughout the summer, as Chl*a* increased, diatoms decreased their total transcript numbers (34.1%) (Fig. 2b), whereas haptophytes changed in abundance (38.4%), with Phaeocystales (*Phaeocystis*) becoming the most active eukaryotic primary producers during both day (65.3%) and night (86.4%). Moreover, during the nocturnal time at the increased Chl*a* period, alveolates were exclusively represented by the Ciliophora from the genus *Stylonychia,* representing up to 63.1% of the total abundance of transcript reads (Fig. 2b).

### Daily *in situ* inorganic C and N assimilation rates and associated active microbes

C-assimilation rates were higher in incubations exposed to light compared to dark incubations, during both Chl*a* sampling periods. On average, C-assimilation rates under light exposure were 723 ± 49 nmol L^{-1} d^{-1} during February, the lower Chl*a* period, compared to 2516 ± 397 nmol L^{-1} d^{-1} during March, with higher Chl*a* (Fig. 3; Supplementary Data, Table S1); this represents an 3.5-fold increase (P < 0.001) throughout the season. Moreover, C-assimilation in dark conditions increased 2.7-fold during the period of higher Chl*a* (1804 ± 171 nmol L^{-1} d^{-1}) compared to the lower Chl*a* period (651 ± 359 nmol L^{-1} d^{-1}); however, these results were not significant (P < 0.895).

Gene markers associated with photosynthesis, the Calvin-Benson cycle and 3-hydroxypropionate bicycle (3-HP) were iden-

tified using metatranscriptomes to define different strategies of active microbial CO$_2$ fixation between the contrasting summer periods (Fig. 4a). The results indicated that although photosynthesis occurred throughout the entire sampling period, it was three times higher (P < 0.7) during the higher Chl*a* period. In contrast, the Calvin-Benson cycle was responsible for the majority of C-assimilation, and was three times higher (P < 0.6) than the 3-HP pathway. The higher transcript numbers associated with C-assimilation observed diurnally could be correlated with the 3-fold increase in carbon incorporation rates observed during light incubations in March (Fig. 3).

In order to correlate photosynthesis with specific active microbial taxa during both sampling periods, transcripts associated with the *psb*A gene (D1 protein of photosystem II) were identified. Gene transcripts were associated with 2.5% of bacteria and 97.5% of eukaryotes (Fig. 4b). Among bacteria, all transcripts were affiliated with Cyanobacteria, such as *Chroococcidiopsis* and *Microcoleus*, during the period of lower Chl*a*, and with *Leptolyngbya* and *Synechococcus* during the period of higher Chl*a* (Fig. 4; Supplementary Data, Table S2). Among eukaryotes, cryptophytes, such as the *Guillardia* genera (70%–100% identity), haptophytes from genus *Phaeocystis* (78% identity) and several members of Bacillariophyta (51% identity) (e.g. *Thalassiosira* and *Fragilariopsis*) were dominant during both sampling periods. Cryptophyta is the most photosynthetically active eukaryote during the summer period.

The Calvin cycle, here represented by the *rbc*L gene (a subunit of ribulose bisphosphate carboxylase), showed similar patterns to the *psb*A gene. Bacteria represented only 0.38% of transcripts and were mostly associated with Proteobacteria and Fusobacteria (*Fusobacterium*), with 99.6% of the transcripts affiliated with the same active eukaryotic groups observed in photosynthesis (Supplementary Data, Table S2). During this cycle, Bacillariophyta and cryptophyte transcript numbers increased 4.7 and 2.9 times, respectively, indicating increased activity during periods of higher Chl*a* (Fig. 4b). Thus, cryptophytes were also the most active eukaryotes related to CO$_2$ fixation processes during the
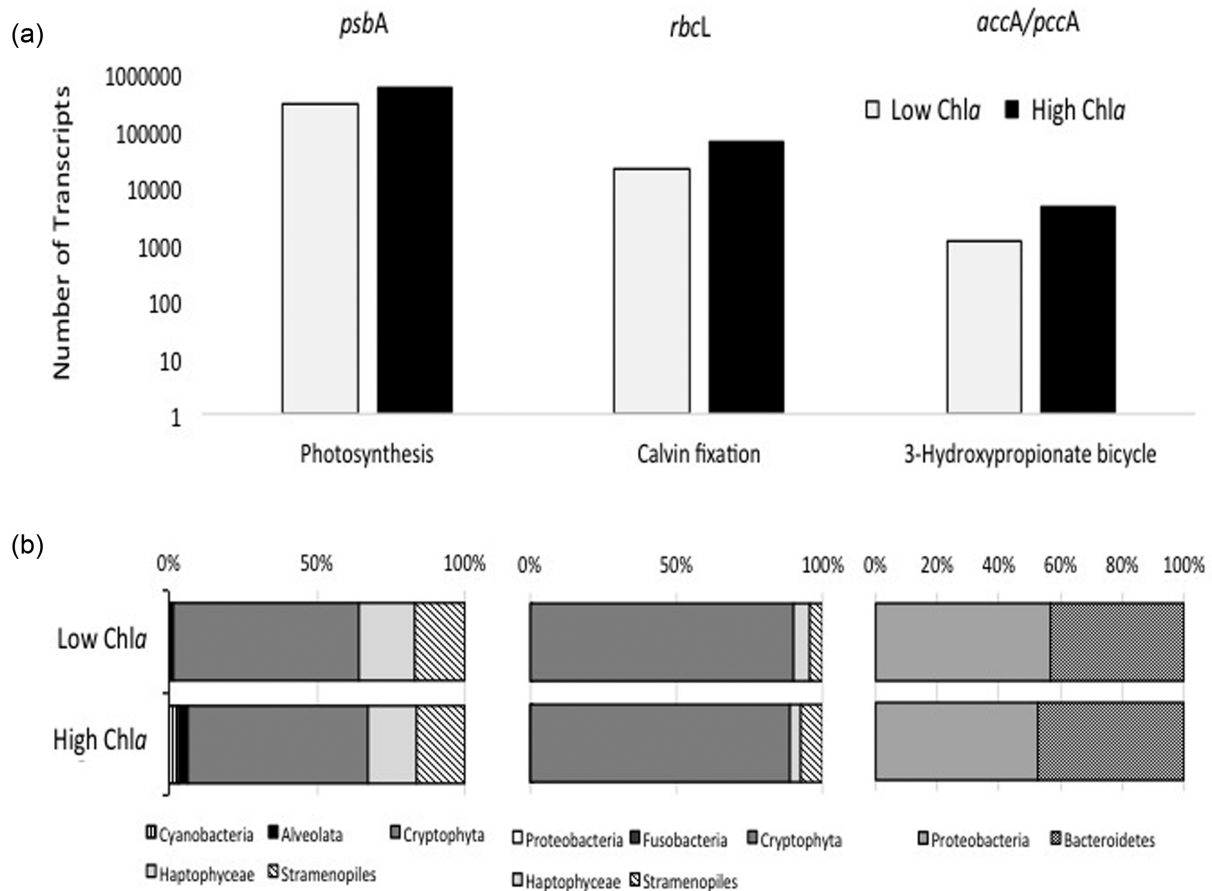
Figure 4. Principal pathways of carbon acquisition and taxonomy between the two sampling periods, higher and lower Chl*a*. (**a**) Transcripts number of mean C associated genes (*psb*A: Photosynthesis; *rbc*L: Calvin Benson cycle; *acc*A and *psa*A:3-Hidroxypropionte bicycle), and (**b**) associated active microbial members responsible for each route.

summer sampling period. Moreover, only 1% of C-assimilation was associated with 3-HP, determined by the *acc*A (Acetil-CoA carboxylase) and *pcc*A (Propionyl-CoA carboxylase) gene markers. These are associated with gamma-proteobacteria (e.g. *Pseudomonas*) and Bacteroidetes (e.g. *Flavobacterium*) (Fig. 4b; Supplementary data, Table S2); and presented no variation between distinct Chl*a* periods.

Contrary to C-assimilation, inorganic N-assimilation (i.e. NH_4^+ and NO_3^-) rates had two to three times greater uptake values in the dark bottles compared incubations exposed to light. There was no significant difference ($P < 0.558$) between samples collected during different Chl*a* periods (Fig. 3; Supplementary Data, Table S1). NO_3^- assimilation rates were an order of magnitude higher ($P = 1$) than NH_4^+ assimilation rates. The average NO_3^- assimilation rate increased from 258 ± 5.7 in February to 706 ± 43.5 nmol L^{-1} d^{-1} in March.

Subsequently, the assimilation of both NH_4^+ and NO_3^- into biomass was evaluated according to the total *gln*A and *nar*B gene transcripts, respectively, obtained from metatranscriptomes (Fig. 5a). Functional taxonomic associations were identified during both periods of higher and lower Chl*a* (Fig. 5b). In general, both *gln*A and *nar*B transcript numbers increase 2-fold to 3-fold ($P < 0.9$) during the period of higher Chl*a*, as well as the registered N-incorporation rates (Fig. 3). Contrary to C-assimilation processes, dominated by eukaryote activity (>90%) as well as active bacteria (<10%), Bacteria and Archaea represented the most active organisms in nitrogen

routes. The only exception was for NO_3^- assimilation, where Bacillariophyta had a low (0.8%) but active presence during the higher Chl*a* period (Fig. 5b). Bacteria, Proteobacteria and Bacteroidetes were the major groups involved in the N-assimilatory routes. Alphaproteobacteria (e.g. Candidatus *Pelagibacter*) and Gammaproteobacteria (e.g. *Pseudoalteromonas*) were responsible for ∼ 99.9% of NH_4^+ assimilation (Supplementary Data, Table S2). In contrast, *Alteromonas*, *Marinobacter*, *Alcanivorax* and *Pseudoalteromonas* (Proteobacteria) as well as *Polaribacter* and *Flavobacterium* (Bacteroidetes) contributed a total of 99.1% to NO_3^- uptake (Supplementary Data, Table S2). Finally, according to the number of total *amo*A gene transcripts obtained from metatranscriptomes, Thaumarchaeota, specifically members of genus *Nitrosopumilus*, contributed to 100% of the nitrification process (Supplementary data; Fig. S4).

DISCUSSION

Chile Bay is the main inlet of Greenwich Island. There is limited information available on oceanographic parameters and processes within this Bay (Cornejo and Arcos 1990; Torres *et al.* 2006). In general, circulation is influenced by bottom topography and wind patterns, resulting in a short water residence time. Water enters from Bransfield Strait into the subsurface over the western side, and leaving superficially on the eastern side (Cornejo and Arcos 1990). Despite the fact that no CTD data were collected from the sampling site in Chile Bay during the
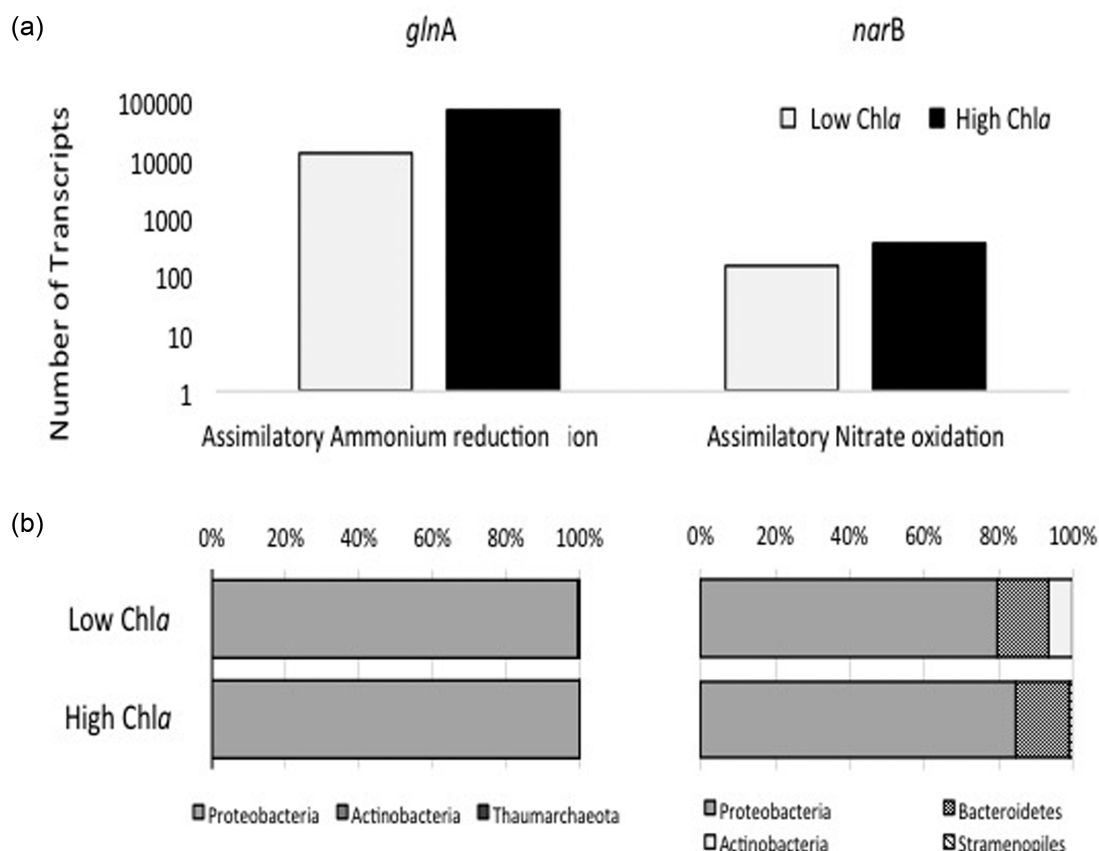
Figure 5. Mean pathways for nitrogen assimilation and its associate taxonomy during both sampling periods, higher and lower Chl*a*. (**a**) Transcripts number of mean genes (*gln*A: Ammonium oxidation; *nar*B: nitrate reduction), and (**b**) associated active microbial members responsible for each route.

summer of 2014, subsequent CTD data taken at the same site in the summer 2017 indicate that there is no marked halocline within the top 50 m of the water column. Moreover, Chile Bay appears to be subjected to ongoing scenarios of accelerated ice melt, due to climate change (Pritchard *et al.* 2012), making the site a reference for improving understanding of how biological processes, driven by microbial communities, respond to environmental changes.

Environmental variables change throughout the austral summer. During the summer of 2014, the air and surface water temperature in Chile Bay were similar to those recorded within other WAP regions (Meredith and King 2005), and salinity (33.1–33.9) was also consistent with other records within the WAP (Meredith and King 2005; Trimborn *et al.* 2015). Within Chile Bay, inorganic nitrogen, nutrients and HPO_4^{2-} levels were similar to levels recorded in regions close to the WAP (Schloss and Ferreyra 2002; Mendes *et al.* 2012, 2013; Trimborn *et al.* 2015). In addition, the dissolved inorganic N:P ratio found was close to the expected regional Redfield ratio (12:1) reported for WAP. Over the WAP continental shelf, nutrients are supplied to the upper ocean via upwelling and mixing of Circumpolar Deep Waters (CDW) (Prézelin *et al.* 2004). Additionally, $[NO_3^-]/[PO_4^{3-}]$ ratios were similar to reports for northern Marguerite Bay by Henley *et al.* (2017), identifying that nutrients supplied to the surface ocean from Upper CDW, with an N:P ratio of 12.9 ± 0.9, coincides with the ratio taken up by phytoplankton in the productive upper ocean. This also coincides with nutrient distribution models from the SO surface waters (Arrigo

et al. 1999; Weber and Deutsch 2010), where there is an established N:P ratio of 12:1, compared with an N:P ratio of 20:1 in the sub-Antarctic zone; these ratio variations are governed by the biogeographic differences in planktonic species composition and biological N utilisation (Weber and Deutsch 2010). High $Si(OH)_4$ concentrations reported in this study agree with the levels found in the Southern Polar Front. The observed low N:Si ratio suggests a relation between the presence of diatoms throughout the entire summer period, as they are the only algae family that build silica-based frustules (Weber and Deutsch 2010).

The increase of Chl*a* towards the end of the 2014 summer, jointly with the apparent consumption of nutrients through biological activities, as well as O_2 production via photosynthesis, suggests the fact that a bloom event occurred during the March sampling in Chile Bay. Samples were composed mainly by diatoms and small flagellates, such as cryptophytes and haptophytes. This coincides with previous reports of late summer phytoplankton blooms in the northern WAP subregion, where Chl*a* contents greater than 5 mg m^{-3} were observed (Montes-Hugo *et al.* 2009). The relatively low accumulation of biomass with respect to other coastal systems may be due to differences in the residence times within semi-enclosed systems (Dellapenna, Kuehl and Schaffner 1998). In Chile Bay, strong surface currents are observed (up to 40 cm s^{-1}), as well as wind-driven water circulation (Cornejo and Arcos 1990; Fuentes *et al.* submitted). This may lead to the exportation of biomass to adjacent waters outside of the bay, a mechanism that has been suggested to control phytoplanktonic bloom growth and

duration (Brandini and Rebello 1994; Schloss *et al.* 1997; Rozema *et al.* 2017a,b). Finally, the observed phytoplankton composition from this study agrees with previous reports, and is closely dependent on the annual and interannual ice cover cycle, as well as on the availability of hours of daylight and the mixed layer depth (Schloss *et al.* 1997; Schloss, Ferreyra and Curtosi 1998; Smith *et al.* 2008; Venables, Clarke and Meredith 2013; Rozema *et al.* 2017b).

Phytoplankton bloom control on microbial community structure and activity

The microbial structure of near surface seawater in Chile Bay during the austral summer followed a similar pattern to nearby regions (Murray *et al.* 1998; Zeng *et al.* 2012). Bacteria were the most abundant domain, and Archaea represented only 1% of the total picoplankton assemblage (Church *et al.* 2003). In Chile Bay, bacteria mostly belong to Proteobacteria and Bacteroidetes, as similarly observed in other polar regions (Malmstrom *et al.* 2007; Galand *et al.* 2009; Alonso-Sáez *et al.* 2010; Bowman *et al.* 2012; Zeng *et al.* 2012).

Although bacterioplankton populations in Chile Bay vary slightly over different production periods, major active orders and classes remained similar throughout the season. Also, C- and N-assimilation activities by bacterioplankton remained low compared to eukaryotes with peak photoautotrophic activities during the period of high Chl*a*. These phototrophic eukaryotes have the ability to sustain the entire food web, as previously suggested for the summer season in the SO (Weber and El-Sayed 1987; Loeb *et al.* 1997; Saba *et al.* 2014). Furthermore, the ubiquity and high transcript numbers retrieved for diatoms, such as *Fragilariopsis,* as well as of cryptophytes, such as *Guillardia*, during the entire sampling period could indicate a potential future impact of increasing sea ice and glacial melt during the summer period, as these eukaryotic members are known to be closely related to ice environments (Moline *et al.* 2004; Schofield *et al.* 2017).

Haptophytes, such as *Phaeocystis antarctica*, were also abundant in Chile Bay and are ubiquitous bloom-forming microorganism in these coastal waters (Schoemann *et al.* 2005; Delmont *et al.* 2014). *Phaeocystis* blooms significantly impact the local nutrient and sulphur budget, impacting their relevant cycles (Van Boekel and Stefels 1993; Yager *et al.* 2012). Furthermore, blooms strongly influence the bacterial community structure in Antarctica (Delmont *et al.* 2014). In accordance with this study, during the high productivity period, the highly abundant and active *Phaeocystis* seem to coexist with bacterial taxa, such as *Polaribacter* (Bacteroidetes) and *Pelagibacter* (Proteobacteria) (Delmont *et al.* 2014).

In addition to Bacillariophyta, cryptophytes and haptophytes (mainly Phaeocystales), relative abundance and activity of alveolates (mainly Ciliophora and Dinophyceae) increased throughout the summer sampling period, and reached its maximum in March. In particular, ciliates have been reported as an important predation pressure on phytoplankton blooms (Schofield *et al.* 2017), which leads to a significant increase in activity during dark periods (i.e. nocturnal) in Chile Bay, whereas diatoms and smaller-sized phytoplankton populations decrease. In the SO, small zooplankton, such as heterotrophic flagellates (Dinophyceae) and ciliates, carry out important biological control activities on phytoplankton (and bacterioplankton). Additionally, grazing from vertical migration has also been noted (Le Quéré *et al.* 2016). The potential increase in grazing activity by Alveolata on phytoplankton may represent an important

process in the reduction of phytoplankton bloom biomass in Chile Bay as well as in other regions of the SO (Ratti, Knoll and Giordano 2013).

Summer production driven by carbon and nitrate and ammonium assimilation

In general, high productivity has been found along the WAP, with average integrated primary production rates varying from 600 mg C m^{-2} d^{-1} during summer phytoplankton blooms (El-Sayed and Taguchi 1981; Arrigo, van Dijken and Bushinsky 2008) up to 7000 mg C m^{-2} d^{-1} within the coastal zone of the Northern Marguerite Bay (Rozema *et al.* 2017a). In Chile Bay, similar to WAP (Anvers Island) (Williams *et al.* 2012), the relatively high observed autotrophic carbon assimilation was driven by the activity of oxygenic photoautotrophs, such as Cryptophyta (i.e. the main active representative in terms of photosynthesis and CO$_2$ fixation), Haptophyta and Bacillariophyta. In addition, carbon fixation using the 3-hydroxypropionate bicycle, assigned to chemoautotrophic microorganisms (dark C-assimilation), primarily Gammaproteobacteria (*Pseudomonas*) and some CFB (Cytophaga-Flavobacterium-Bacteroides) members, contributed <1% of the total C-assimilation, compared to >99% of light-dependent C-fixation performed by phytoplankton. Dark C-assimilation by these two groups of organisms is both important to and relevant for the total carbon cycle budget in this extreme marine ecosystem.

With respect to N assimilation, the literature suggests that small phytoplankton exhibited a greater preference for NH$_4^+$ compared to than large diatoms (Owens, Priddle and Whitehouse 1991; Bode *et al.* 2002). The findings from Chile Bay revealed high numbers of nocturnal *gln*A transcripts with respect to *nar*B genes. However, NH$_4^+$-assimilation rates are five times lower than NO$_3^-$ assimilation rates, suggesting that NH$_4^+$ is being used at the same rate it is being produced by Proteobacteria, which appear to be the most active microbes in this process. Tupas *et al.* (1993) reported that 8%–25% of the total NH$_4^+$ uptake in Antarctic coastal water is associated with bacterial activity during a phytoplankton bloom. In this case, the 2014 microbial bloom registered for Chile Bay demonstrated the presence of organisms that preferentially assimilate NO$_3^-$, or use both nitrate and ammonium as nitrogen sources (Lancelot, Mathot and Owens 1986). This is contrary to reports from natural assemblages, where phytoplankton consistently prefers to use NH$_4^+$ rather than NO$_3^-$. Studies have indicated that instead of a gradual change from NO$_3^-$-based to NH$_4^+$-based production during summer (Tamminen 1995), secondary blooms may develop in areas such as the Western Bransfield Strait that use NO$_3^-$ as a predominant nitrogen source (Bode *et al.* 2002). This NO$_3^-$ preference coincides with the high NO$_3^-$ concentrations reported in the WAP for near-surface open-ocean waters. However, it should be considered that locally recycled NH$_4^+$ (high turnover time) may also make an important contribution to phytoplankton nutrition, mostly associated with smaller-sized phytoplankton.

In addition, nitrification processes may be an important source of recycled NO$_3^-$ to the primary production budget in the WAP. In fact, Archaeal ammonia oxidation has provided contributions of 3%–6% of annual primary production by chemoautotrophic carbon fixation (Tolar *et al.* 2016). In Chile Bay, active nitrification process by Thaumarchaeota, from the genus *Nitrosopumilus,* was indicated by the presence of transcripts of the *amo*A gene (Supplementary data, Fig. S4). In the future, it is

important to gain an improved understanding of the nitrification contribution to primary production in Chile Bay, as well as secondary N_2O production, especially when an undersaturation of N_2O has been recently reported in polar waters, such as those from the polar mixed layer at the Arctic Ocean (Verdugo *et al.* 2016).

CONCLUSIONS

Chile Bay is a dynamic system subjected to ongoing ice melt caused by climate change. This is also the case for other coastal areas within WAP. Therefore, Chile Bay functions as a good reference to further understanding of microorganism response under these conditions.

Phytoplankton bloom of active diatoms and small flagellates, such as members of cryptophytes and haptophytes, during the summer (i.e. February and March) were accompanied by an increase of Chl*a* of up to 2.5 mg m^{-3}, reflecting active biological production by photoautotrophs that could potentially sustain the food web during summer.

Phototrophic light-dependent C-fixation accounted for up to 99% of total C-assimilation, whereas darkness-dependent C-fixation accounting for <1%. These relatively high rates of primary production based on carbon (photosynthesis, Calvin-Benson and 3-HP), compared to temperate waters such as in the Pacific Ocean, were by >90% associated with eukaryotes (cryptophytes, haptophytes and diatoms) and <10% associated with Bacteria (Cyanobacteria, Fusobacteria, Proteobacteria and Bacteroidetes). Proteobacteria and Bacteroidetes were the most active microbes in NH_4^+ and NO_3^- assimilations.

Grazing of Alveolates (mainly members of Ciliophora) during nocturnal vertical migration plays a potentially important role biologically on controlling phytoplankton (and bacterioplankton). Within the region, variations in phytoplankton biomass, composition and size caused by climate change (and mixing within the water column) may impact grazers as well as higher trophic levels in the food web.

SUPPLEMENTARY DATA

Supplementary data are available at *FEMSLE* online.

ACKNOWLEDGEMENTS

FUNDING

REFERENCES

Alonso-Sáez L, Galand PE, Casamayor EO *et al.* High bicarbonate assimilation in the dark by Arctic bacteria. *ISME J* 2010;**4**:1581–90.

Anders S, Huber W. Differential expression analysis for sequence count data. *Genome Biol* 2010;**11**:106.

Andrews S. FastQC: a quality control tool for high through-put sequence data. 2010. http://www.bioinformatics.babraham.ac.uk/projects/fastqc.

Arblaster JM, Meehl GA, Karoly DJ. Future climate change in the Southern Hemisphere: competing effects of ozone and greenhouse gases. *Geophys Res Lett* 2011. doi:10.1029/2010GL045384.

Arrigo KR, Robinson DH, Worthen DL *et al.* Phytoplankton community structure and the drawdown of nutrients and CO_2 in the Southern Ocean. *Science* 1999;**283**:365–7.

Arrigo KR, van Dijken GL, Bushinsky S. Primary production in the Southern Ocean, 1997–2006. *J Geophys Res* 2008;**113**:C08004.

Bode A, Castro CG, Doval MD *et al.* New and regenerated production and ammonium regeneration in the western Bransfield Strait region (Antarctica) during phytoplankton bloom conditions in summer. *Deep-Sea Res Pt II* 2002;**49**:787–804.

Borges-Mendes CR, Silva de Souza M, Tavano Garcia VM. Dynamics of phytoplankton communities during late summer around the tip of the Antarctic Peninsula. *Deep-Sea Res Pt I* 2012;**65**:1–14.

Borges-Mendes CRTavano VM, Leal MC *et al.* Shifts in the dominance between diatoms and cryptophytes during three late summers in the Bransfield Strait (Antarctic Peninsula). *Polar Biol* 2013;**36**:537–47.

Bowman JS, Rasmussen S, Blom N *et al.* Microbial community structure of Arctic multiyear sea ice and surface seawater by 454 sequencing of the 16S RNA gene. *ISME J* 2012;**6**:11–20.

Buchan A, LeCleir GR, Gulvik CA *et al.* Master recyclers: features and functions of bacteria associated with phytoplankton blooms. *Nat Rev Microbiol* 2014;**12**:686–98.

Buchfink B, Xie C, Huson DH. Fast and sensitive protein alignment using DIAMOND. *Nat Methods* 2015;**12**:59–60.

Bunse C, Pinhassi J. Marine bacterioplankton seasonal succession dynamics. *Trends Microbiol* 2017;**25**:494–505.

Brandini FP, Rebello J. Wind field effect on hydrography and chlorophyll dynamics in the coastal pelagial of Admiralty Bay, King George Island, Antarctica. *Antarct Sci* 1994;**6**:433–42.

Cavicchioli R. Microbial ecology of Antarctic aquatic systems. *Nat Rev Microbiol* 2015;**13**:691–706.

Church M, DeLong E, Ducklow H *et al.* Abundance and distribution of planktonic Archaea and Bacteria in the waters west of the Antarctic Peninsula. *Limnol Oceanogr* 2003;**48**:1893–902.

Cornejo M, Arcos F. Estudio de algunas características físicas y biológicas de la columna de agua en Bahía Chile-Isla Greenwich. *Acta Antártica Ecuatoriana, PROANTEC, Ecuador* 1990;**2**:21–7.

Delmont TO, Hammar KM, Ducklow HW *et al.* Phaeocystis antarctica blooms strongly influence bacterial community structures in the Amundsen Sea polynya. *Front Microbiol* 2014;**5**:1–13.

Dellapenna TM, Kuehl SA, Schaffner LC. Sea-bed mixing and particle residence times in biologically and physically dominated estuarine systems: a comparison of lower Chesapeake Bay and the York River subestuary. *Estuar Coast Shelf S* 1998;**46**:777–95.

Deppeler S, Davidson AT. Southern ocean phytoplankton in a changing climate. *Front Mar Sci* 2017;**4**:40.

Díez B, Pedrós-Alió C, Massana C. Study of genetic diversity of eukaryotic picoplankton in different oceanic regions by Small-Subunit rRNA gene cloning and sequencing. *Appl Environ Microb* 2001;**67**:2932–41.

Ducklow H, Clarke A, Dickhut R *et al.* The marine system of the Western Antarctic Peninsula. In: Rogers AD, Johnston NM, Murphy EJ *et al* (eds.) *Antarctic Ecosystems: An Extreme Environment in a Changing World.* Blackwell Publishing Ltd: Oxford, UK, 2012, 121–59.

Ducklow H, Fraser W, Meredith M *et al.* West Antarctic Peninsula: An ice-dependent coastal marine ecosystem in transition. *Oceanography* 2013;**26**:190–203.

Ducklow HW, Baker K, Martinson DG *et al.* Marine pelagic ecosystems: the West Antarctic Peninsula. *Philos T Roy Soc B Biol Sci* 2007;**362**:67–94.

Dugdale RC, Wilkerson FP. The use of ^{15}N to measure nitrogen uptake in eutrophic oceans; experimental considerations. *Limnol Oceanogr* 1986;**4**, doi:10.4319/lo.1986.31.4.0673.

Egas C, Henríquez-Castillo C, Delherbe N *et al.* Short timescale dynamics of phytoplankton in Fildes Bay, Antarctica. *Antarct Sci* 2017;**29**:1–12.

El-Sayed SZ, Taguchi S. Primary production and standing crop of phytoplankton along the ice-edge in the Weddell Sea. *Deep-Sea Res A* 1981;**9**:1017–32.

Evans C, Brandsma J, Pond DW *et al.* Drivers of interannual variability in virioplankton abundance at the coastal Western Antarctic Peninsula and the potential effects of climate change. *Environ Microbiol* 2017;**19**:740–55.

Fan T, Deser C, Schneider DP. Recent Antarctic sea ice trends in the context of Southern Ocean surface climate variations since 1950. *Geophys Res Lett* 2014;**41**:2419–26.

Fernandez C, Farías L, Alcamán ME. Primary production and nitrogen regeneration processes in surface waters of the Peruvian upwelling system. *Progr Oceanogr* 2009;**83**:159–68.

Field CB, Behrenfeld MJ, Randerson JT *et al.* Primary production of the biosphere: integrating terrestrial and oceanic components. *Science* 1998;**281**:237–40.

Finkel ZV, Beardal IJ, Flynn KJ *et al.* Phytoplankton in a changing world: cell size and elemental stoichiometry. *J Plankton Res* 2010;**32**:119–37.

Frölicher TL, Rodgers KB, Stock CA *et al.* Sources of uncertainties in 21st century projections of potential ocean ecosystem stressors. *Global Biogeochem Cycles* 2016;**30**: 1224–43.

Fuentes S, Arroyo JI, Rodríguez-Marconi S *et al.* Short-term dynamics of summer phyto- and bacterioplankton communities in Chile Bay, Antarctic Peninsula. *Polar Biol*, submitted

Galand PE, Casamayor EO, Kirchman DL *et al.* Ecology of the rare microbial biosphere of the Arctic Ocean. *P Natl Acad Sci USA* 2009;**106**:22427–32.

Garibotti IA, Vernet M, Ferrario ME. Annually recurrent phytoplanktonic assemblages during summer in the seasonal ice zone west of the Antarctic Peninsula (Southern Ocean). *Deep-Sea Res Pt I* 2005;**52**:1823–41.

Giovannoni SJ, Vergin KL. Seasonality in ocean microbial communities. *Science* 2012;**335**:671–6.

Gonçalves-Araujo R, Silva de Souza M, Tavano VM *et al.* Influence of oceanographic features on spatial and interannual variability of phytoplankton in the Bransfield Strait, Antarctica. *J Mar Syst* 2015;**142**:1–15.

Grzymski JJ, Riesenfeld CS, Williams TJ *et al.* A metagenomic assessment of winter and summer bacterioplankton from Antarctica Peninsula coastal surface waters. *ISME J* 2012;**6**:1901–15.

Hauri C, Doney SC, Takahashi T *et al.* Two decades of inorganic carbon dynamics along the West Antarctic Peninsula. *Biogeosciences* 2015;**12**:6761–79.

Hawkings JR, Wadham JL, Tranter M *et al.* Ice sheets as a significant source of highly reactive nanoparticulate iron to the oceans. *Nat Commun* 2014;**5**:3929.

Hallegraeff GM. Ocean climate change, phytoplankton community responses, and harmful algal blooms: a formidable predictive challenge. *J Phycol* 2010;**46**:220–35.

Henley SF, Ganeshram RS, Annett AL *et al.* Macronutrient supply, uptake and recycling in the coastal ocean of the west Antarctic Peninsula. *Deep Sea Res Part II Top Stud Oceanogr* 2017;**139**:58–76.

Huson DH, Auch AF, Qi J *et al.* MEGAN analysis of metagenomic data. *Genome Res* 2007;**17**:377–86.

Joubert WR, Thomalla SJ, Waldron HN *et al.* Nitrogen uptake by phytoplankton in the Atlantic sector of the Southern Ocean during late austral summer. *Biogeosciences* 2011;**8**:2947–59.

Kavanaugh MT, Abdala FN, Ducklow HW *et al.* Effect of continental shelf canyons on phytoplankton biomass and community composition along the western Antarctic Peninsula. *Mar Ecol Prog Ser* 2015;**524**:11–26.

Kirchman DL, Stegman MR, Nikrad MP *et al.* Abundance, size, and activity of aerobic anoxygenic phototrophic bacteria in coastal waters of the West Antarctic Peninsula. *Aquat Microb Ecol* 2014;**73**:41–9.

Koike I, Holm-Hansen O, Biggs DC. Inorganic nitrogen metabolism by Antarctic phytoplankton with special reference to ammonium cycling. *Mar Ecol Prog Ser* 1986;**30**:105–16.

Kopczyńska EE, Fiala M, Jeandel C. Annual and interannual variability in phytoplankton at a permanent station off Kerguelen Islands, Southern Ocean. *Polar Biol* 1998;**20**:342–51.

Kopylova E, Noé L, Touzet H. SortMeRNA: fast and accurate filtering of ribosomal RNAs in metatranscriptomic data. *Bioinformatics* 2012;**28**:3211–7.

Korb RE, Whitehouse MJ, Gordon M *et al.* Summer microplankton community structure across the Scotia Sea: implications for biological carbon export. *Biogeosciences* 2010;**7**:343–56.

Lancelot C, Mathot S, Owens NJ. Modelling protein synthesis, a step to an accurate estimate of net primary production: phaeocystis pouchetii colonies in Belgian coastal waters. *Mar Ecol Prog Ser* 1986;**32**:193–202.

Le Quéré C, Buitenhuis ET, Moriarty R *et al.* Role of zooplankton dynamics for Southern Ocean phytoplankton biomass and global biogeochemical cycles. *Biogeosciences* 2016;**13**:4111–33.

Le Quéré C, Rodenbeck C, Buitenhuis ET *et al.* Saturation of the Southern Ocean CO_2 sink due to recent climate change. *Science* 2007;**316**:1735–8.

Loeb V, Siegel V, Holm-Hansen O *et al.* Effects of sea-ice extent and krill or salp dominance on the Antarctic food web. *Nature* 1997;**38**,897.

Luria CM, Amaral-Zettler LA, Ducklow HW *et al.* Seasonal succession of free-living bacterial communities in coastal waters of the Western Antarctic Peninsula. *Front Microbiol* 2016;**3**: 1731.

McKie-Krisberg ZM, Gast RJ, Sanders RW. Physiological responses of three species of Antarctic mixotrophic phytoflagellates to changes in light and dissolved nutrients. *Microb Ecol* 2015;**70**:21–9.

Malmstrom RR, Straza T, Cottrell MT *et al.* Diversity, abundance, and biomass production of bacterial groups in the western Arctic Ocean. *Aquat Microb Ecol* 2007;**47**:45–55.

Martin M. Cutadapt removes adapter sequences from high-throughput sequencing reads. *EMBnet J* 2011;**17**:1–10.

Mendes CRB, de Souza MS, Garcia VMT *et al*. Dynamics of phytoplankton communities during late summer around the tip of the Antarctic Peninsula, *Deep Res Part I Oceanogr Res Pap* 2012;**65**:1–14.

Meredith MP, King JC. Rapid climate change in the ocean west of the Antarctic Peninsula during the second half of the 20th century. *Geophys Res Lett* 2005;**32**:L19604.

Metzl N, Tilbrook B, Poisson A. The annual fCO_2 cycle and the air-sea CO_2 flux in the sub-Antarctic Ocean. *Tellus B* 1999;**51**: 849–61.

Moline MA, Claustre H, Frazer TK *et al*. Alteration of the food web along the Antarctic Peninsula in response to a regional warming trend. *Global Change Biol* 2004;**10**:1973–80.

Montes-Hugo M, Doney SC, Ducklow HW *et al*. Recent changes inphytoplankton communities associated with rapid regional climate change along the western Antarctic Peninsula. *Science* 2009;**323**:1470–3.

Montes-Hugo M, Vernet M, Martinson D *et al*. Variability on phytoplankton size structure in the western Antarctic Peninsula (1997–2006). *Deep-Sea Res Pt II* 2008;**55**:2106–17.

Moorthi SD, Caron DA, Gast R *et al*. Mixotrophy: a widespread and important ecological strategy for planktonic and sea-ice nanoflagellates in the Ross Sea, Antarctica. *Aquat Microb Ecol* 2009;**54**:269–77.

Murray AE, Preston CM, Massana R *et al*. Seasonal and spatial variability of bacterial and archaeal assemblages in the coastal waters near Anvers Island, Antarctica. *Appl Environ Microb* 1998;**64**:2585–95.

Olson RJ. Nitrate and ammonium uptake in Antarctic waters. *Limnol Oceanogr* 1980;**25**:1064–1.

Owens NJP, Priddle J, Whitehouse MJ. Variations in phytoplanktonic nitrogen assimilation around South Georgia and in the Bransfield Strait (Southern Ocean). *Mar Chem* 1991;**35**:287–304.

Pearson GA, Lago-Leston A, Canovas F *et al*. Metatranscriptomes reveal functional variation in diatom communities from the Antarctic Peninsula. *ISME J* 2015;**9**:2275–89.

Peck LS, Barnes DKA, Cook AJ *et al*. Negative feedback in the cold: Ice retreat produces new carbon sinks in Antarctica. *Glob Change Biol* 2010;**16**:2614–23.

Petlicki M, Kinnard C. Calving of Fuerza Aérea Glacier (Greenwich Island, Antarctica) observed with terrestrial laser scanning and continuous video monitoring. *J Glaciol* 2016;**62**: 835–46.

Piquet AMT, Bolhuis H, Meredith MP *et al*. Shifts in coastal Antarctic marine microbial communities during and after melt water-related surface stratification. *FEMS Microbiol Ecol* 2011;**76**:413–27.

Prézelin BB, Hofman EE, Mengelt C *et al*. The linkage between upper circumpolar deepwater (UCDW) and phytoplankton assemblages on the west Antarctic Peninsula continental shelf. *J Mar Res* 2000;**58**:165–202.

Prézelin BB, Hofmann EE, Moline M *et al*. Physical forcing of phytoplankton community structure and primary production in continental shelf waters of the Western Antarctic Peninsula. *J Mar Res* 2004;**62**:419–60.

Pritchard HD, Ligtenberg SRM, Fricker HA *et al*. Antarctic ice-sheet loss driven by basal melting of ice shelves. *Nature* 2012;**484**:502–5.

Quast C, Pruesse E, Yilmaz P *et al*. The SILVA ribosomal RNA gene database project: improved data processing and web-based tools. *Nucleic Acids Res* 2013;**41**(Database issue):D590–6.

Raimbault P, Slawyk G, Boudjellal B *et al*. Carbon and nitrogen uptake and export in the equatorial Pacific at 150 degrees W: Evidence of an efficient regenerated production cycle. *Geophys Res* 1999;**104**:3341–56.

Ratti S, Knoll AH, Giordano M. Grazers and phytoplankton growth in the oceans: an experimental and evolutionary perspective. *PLoS One* 2013;**8**:e77349.

Redfield AC. The biological control of the chemical factors in the environment. *Am Sci* 1958;**46**:1–18.

Rozema PD, Biggs T, Sprong PA *et al*. Summer microbial community composition governed by upper-ocean stratification and nutrient availability in northern Marguerite Bay, Antarctica. *Deep-Sea Res Pt II* 2017a;**139**:151–66.

Rozema PD, Venables HJ, Poll WH *et al*. Interannual variability in phytoplankton biomass and species composition in northern Marguerite Bay (West Antarctic Peninsula) is governed by both winter sea ice cover and summer stratification. *Limnol Oceanogr* 2017b;**62**:235–52.

Saba GK, Fraser WR, Saba VS *et al*. Winter and spring controls on the summer food web of the coastal West Antarctic Peninsula. *Nat Commun* 2014;**5**:4318.

Sabine CL, Feely RA, Gruber N *et al*. The oceanic sink for anthropogenic CO_2. *Science* 2004;**305**:367–71.

Santana E, Dumont JF. Geologia de los alrededores de la estación ecuatoriana Pedro Vicente Maldonado (Isla Greenwhc) e isla DEE, Península Antártica. *Acta Antártica Ecuatoriana. PROANTEC, Ecuador.* 2002;**1**:7–32.

Smith RC, Martinson DG, Stammerjohn SE *et al*. Bellingshausen and Western Antarctic Peninsula region: pigment biomass and sea ice spatial/temporal distributions and interannual variability. *Deep-Sea Res Pt II* 2008;**55**: 1949–63.

Schloss IR, Ferreyra GA. Primary production, light and vertical mixing in Potter Cove, a shallow bay in the maritime Antarctic. *Polar Biol* 2002;**25**:41–8.

Schloss IR, Ferreyra GA, Curtosi A. Primary production and conditions for phytoplankton growth in Potter Cove, King George Island. In: Wiencke C, Ferreyra GA, Arntz W *et al*. (eds.) *The Potter Cove Coastal Ecosystem, Antarctica. Rep Polar Res*, 1998; **299**: 67–73.

Schloss IR, Kloser H, Ferreyra GA *et al*. Factors governing phytoplankton and particulate matter variation in Potter Cove, King George island, Antarctica. In: Battaglia B, Valencia J, Walton DWH (eds.) *Antarctic Communities*. Cambridge, UK: Cambridge University Press, 1997, 135–41.

Schmale J, Schneider J, Nemitz E *et al*. Sub-Antarctic marine aerosol: dominant contributions from biogenic sources. *Atmos Chem Phys* 2013;**13**:8669–94.

Schoemann V, Becquevorta S, Stefelsb J *et al*. Phaeocystis blooms in the global ocean and their controlling mechanisms: a review. *J Sea Res* 2005;**53**:43–66.

Schofield O, Saba GK, Coleman K *et al*. Decadal variability in coastal phytoplankton community composition in a changing West Antarctic Peninsula. *Deep-Sea Res Pt I* 2017;**124**:42–54.

Slawyk G, Raimbault P. Simple procedure for simultaneous recovery of dissolved inorganic and organic nitrogen in 15N-tracer experiments and improving the isotopic mass balance. *Mar Ecol Prog Ser* 1995;**124**:289–99.

Solorzano L. Determination of ammonia in natural water by the phenolhypochlorite method. *Limmol Oceanogr* 1969;**14**:799–801.

Statham PJ, Skidmore M, Tranter M. Inputs of glacially derived dissolved and colloidal iron to the coastal ocean and implications for primary productivity. *Global Biogeochem Cycles* 2008;**22**:GB3013, DOI:10.1029/2007GB003106.

Steig EJ, Schneider DP, Rutherford SD *et al*. Warming of the Antarctic ice-sheet surface since the 1957 International Geophysical Year. *Nature* 2009;**457**:459–62.

Strickland JDH, Parsons TR. A *Practical Handbook of Seawater Analysis*. 2nd Edition, Fisheries Research Board of Canada Bulletin, No. 167, Fisheries Research Board of Canada, 310, 1972.

Takahashi T, Sutherland SC, Wanninkhof R *et al*. Climatological mean and decadal change in surface ocean pCO_2, and net sea-air CO_2 flux over the global oceans. *Deep-Sea Res Pt II* 2009;**56**:554–77.

Tamminen T. Nitrate and depletion rates and preferences during a Baltic spring bloom. *Mar Ecol Prog Ser* 1995;**120**:123–33.

Tolar BB, Ross MJ, Wallsgrove NJ *et al*. Contribution of ammonia oxidation to chemoautotrophy in Antarctic coastal waters. *ISME J* 2016. DOI:10.1038/ismej.2016.61.

Torres G, Palacios C, Calderón T *et al*. Interacción del fitoplancton y zooplancton y sus condiciones oceanográficas durante el verano austral 2004 (Isla Greenwich-Antártica). *Revista Tecnológica ESPOL* 2006;**19**:153–60.

Tupas LM, Koike I, Karl DM *et al*. Nitrogen metabolism by heterotrophic bacterial assemblages in Antarctic coastal waters. *Polar Biol* 1993;**14**:195–204.

Turner J, Lu H, White I *et al*. Absence of 21st century warming on Antarctic Peninsula consistent with natural variability. *Nature* 2016;**535**:411.

Thomsen J, Johnson KS, Petty RL. Determination of reactive silicate in seawater by flow injection analysis. *Anal Chem* 1983;**55**:2378–82.

Trimborn S, Hoppe CJM, Taylor BB *et al*. Open Ocean and coastal phytoplankton communities of western Antarctic Peninsula and Drake Passage waters. PANGAEA. *Deep-Sea Res Pt I* 2015;**98**:115–24.

Van Boekel JSW, Stefels WHM. Production of DMS from dissolved DMSP in axenic cultures of the marine phytoplankton species *Phaeocystis* sp. *Mar Ecol Prog Ser* 1993;**97**:11–8.

Varela M, Fernandez E, Serret P. Size-fractionated phytoplankton biomass and primary production in the Gerlache and south Bransfield Straits (Antarctic Peninsula) in Austral summer 1995–1996. *Deep-Sea Res Pt II* 2002;**49**:749–68.

Venables HJ, Clarke A, Meredith MP. Wintertime controls on summer stratification and productivity at the western Antarctic Peninsula. *Limnol Oceanogr* 2013;**58**:1035–47.

Verdugo J, Damm E, Snoeijs P *et al*. Climate relevant trace gases (N_2O and CH_4) in the Eurasian Basin (Arctic Ocean). *Deep-Sea Res Pt I* 2016;**117**:84–94.

Vernet M, Martinson D, Iannuzzi R *et al*. Primary production within the sea-ice zone west of the Antarctic Peninsula: I—Sea ice, summer mixed layer, and irradiance, *Deep-Sea Res Pt II* 2008;**55**:2068–85.

Waldron HN, Attwood CG, Probyn TA *et al*. Nitrogen dynamics in the Bellingshausen Sea during the Austral spring of 1992. *Deep-Sea Res Pt II* 1995;**42**:1253–76.

Walsh JJ, Dieterle DA, Lenes J. A numerical analysis of carbon dynamics of the Southern Ocean phytoplankton community: the roles of light and grazing in effecting both sequestration of atmospheric CO_2 and food availability to larval krill. *Deep-Sea Res Pt I* 2001;**48**:1–48.

Wang S, Bailey D, Lindsay K *et al*. *Biogeosciences* 2014;**11**:4713–31.

Weber LH, El-Sayed SZ. Contributions of the net, nano-and picoplankton to the phytoplankton standing crop and primary productivity in the Southern Ocean. *J Plankton Res* 1987;**9**:973–94.

Weber TS, Deutsch C. Ocean nutrient ratios governed by plankton biogeography. *Nature* 2010;**467**:550–4.

Williams TJ, Long E, Evans F *et al*. A metaproteomic assessment of winter and summer bacterioplankton from Antarctic Peninsula coastal surface waters. *ISME J* 2012;**6**:1883–900.

Williams TJ, Wilkins D, Long E *et al*. The role of planktonic Flavobacteria in processing algal organic matter in coastal East Antarctica revealed using metagenomics and metaproteomics. *Environ Microbiol* 2013;**15**:1302–17.

Wilkins D, Yau S, Williams TJ *et al*. Key microbial drivers in Antarctic aquatic environments. *FEMS Microbiol Rev* 2013;**37**:303–35.

Yager PL, Sherrell L, Stammerjohn SE *et al*. ASPIRE: the Amundsen Sea Polynya international research expedition. *Oceanography* 2012;**25**:40–53.

Zeng Y, Yu Y, Qiao Z *et al*. Diversity of bacterioplankton in coastal seawaters of Fildes Peninsula, King George Island, Antarctica. *Arch Microbiol* 2012;**196**:137–47.